Differential transmission and dynamics of pump-excited carriers in graphene

B. Y. Sun, Y. Zhou, and M. W. Wu*

Hefei National Laboratory for Physical Sciences at Microscale and Department of Physics, University of Science and Technology of China, Hefei, Anhui, 230026, China
*Corresponding author: mwwu@ustc.edu.cn

Abstract

We investigate the dynamics of photoexcited carriers and nonequilibrium phonons in graphene by solving the kinetic Bloch equations with the relevant scatterings (including the Coulomb scattering with dynamic screening) explicitly included. Under the gauge invariant approach, both the drift and pump terms are included naturally. We look into the dynamics of carriers under the linear polarized laser pulses with the pump-photon energy in both near-infrared and THz regimes. When the pump-photon energy is high enough, the influence of the drift term is shown to be negligible. Moreover, the anisotropic photoexcited electrons tend to be isotropic under the scattering and an isotropic hot-electron Fermi distribution is established before the end of the pulse investigated here as shown in Fig. 1. However, in the case with low pump-photon energy, the drift term is important which leads to a net momentum transfer from the electric field to electrons. Together with the dominant Coulomb scattering, a drifted Fermi distribution different from the one established under static electric field is found to be established in several hundred femtoseconds. We further show that the Auger process investigated in the literature which involves only the diagonal terms of density matrices, is forbidden by the dynamic screening. However, we propose an Auger process involving the interband coherence and show that it contributes to the dynamics of carriers when the pump-photon energy is low as shown in Fig. 2.

We also investigate the dynamics of the carriers after the pulse. It is shown that the temporal evolutions of the positive differential transmission obtained from our calculations agree with the experiments by Wang *et al.* [1] and Hale *et al.* [2] very well, with two distinct differential transmission relaxations presented (Fig. 3). For these two relaxations, we show that the fast one is due to the rapid carrier-phonon thermalization and the slow one is mainly because of the slow decay of hot phonons.

In addition to the positive differential transmission, the negative one which can appear after the establishment of the Fermi distribution [3,4,5] is also investigated. It is shown that, for intrinsic graphene, the negative differential transmission can appear at low probe-photon energy (in the order of the scattering rate) or at high energy (much larger than the scattering rate). For the low probe-photon energy case, the negative differential transmission is found to come from the increase of the intraband conductivity due to the large variation of electron distribution after the pumping. As for the high probe-photon energy case, the negative differential transmission is shown to tend to appear with the hot-electron temperature being closer to the equilibrium one and the chemical potential higher than the equilibrium one but considerably smaller than half of the probe-photon energy. We also show that this negative differential transmission can come from both the inter- and the intraband components of the conductivity. Especially, for the interband component, its contribution to the negative differential transmission is shown to come from both the Hartree-Fock self-energy and the scattering.

This work was supported by the National Basic Research Program of China under Grant No. 2012CB922002, the National Natural Science Foundation of China under Grant No. 10725417 and the Strategic Priority Research Program of the Chinese Academy of Sciences under Grant No. XDB01000000.

References

[1] H. Wang, J. H. Strait, P. A. George, S. Shivaraman, V. B. Shields, M. Chandrashekhar, J. Hwang, F. Rana, M. G. Spencer, C. S. Ruiz-Varges, and J. Park, Appl. Phys. Lett. **96** (2010), 081917.
[2] P. J. Hale, S. M. Hornett, J. Moger, D. W. Horsell, and E. Hendry, Phys. Rev. B **83** (2011), 121404(R).
[3] J. Shang, Z. Luo, C. Cong, J Lin, T. Yu, and G. G. Gurzadyan, Appl. Phys. Lett. **97** (2010), 163103.
[4] J. Shang, T. Yu, J. Lin, and G. G. Gurzadyan, ACS Nano **5** (2011), 3278.
[5] M. Breusing, S. Kuehn, T. Winzer, E. Malic, F. Milde, N. Severin, J. P. Rabe, C. Ropers, A. Knorr, and T. Elsaesser, Phys. Rev. B **83** (2011), 153410.
[6] B. Y. Sun, Y. Zhou, and M. W. Wu, Phys. Rev. B **85** (2012), 125413.
[7] B. Y. Sun and M. W. Wu, New J. Phys. **15** (2013), 083038.
[8] B. Y. Sun and M. W. Wu, Phys. Rev. B **88** (2013), 235422.

Figures

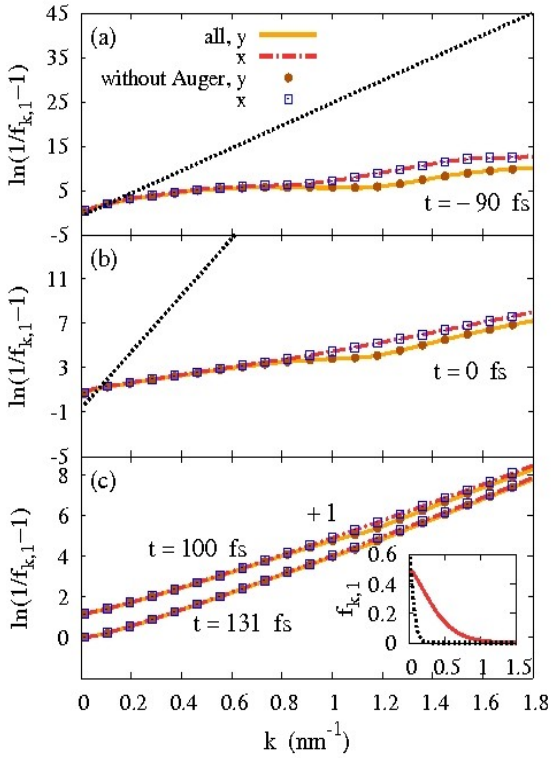

Fig. 1. (a)-(c) $\ln(f_{k,1}-1)$ as function of k along the **x** and **y** directions at t=-90, 0, 100 and 131 fs. Here, $f_{k,1}$ is the distribution function of electrons in conduction band. It is noted that if the Fermi distribution is established, $\ln(f_{k,1}-1)$ becomes a linear function of k. The black dotted curves in (a) and (b) are the case before the pump pulse. The curve for t=100 fs plotted in (c) is $\ln(f_{k,1}-1)+1$. The cases without the Auger process are also plotted in (a)-(c). The comparison of the electron distributions $f_{k,1}$ at t=-100 (black dotted curve) and 131 fs (red solid curve) are plotted in the inset.

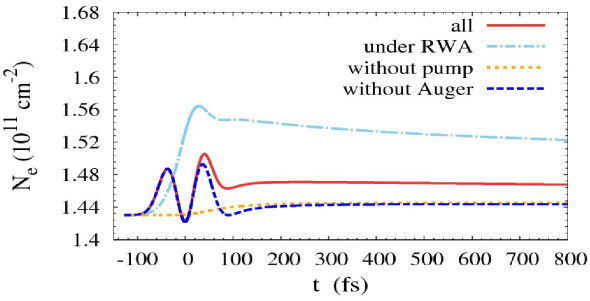

Fig. 2. Temporal evolution of the electron densities for the cases with all the processes included, without Auger process, without pump process and under the rotating-wave approximation, separately. Here, the pump-photon energy is 15 meV.

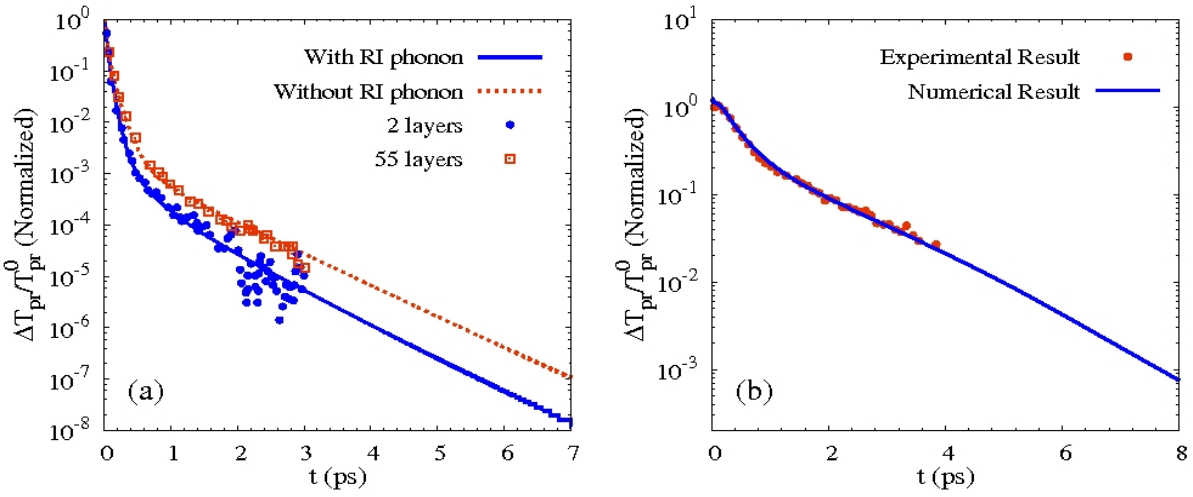

Fig. 3. Differential transmission from the numerical results compared with the experimental results (a) on SiC by Wang *et al.* [1] and on SiO_2 by Hale *et al.* [2].